Electronic Supplementary Material (ESI) for Sustainable Energy & Fuels.

Supporting information

Realizing Favourable Oxygen Electrocatalytic Activity with Compositionally Complex Metal Molybdates

Hemanth Kumar Beere, [†] Pranav Kulkarni, [¥†] Uday Narayan Maiti, [††] R Geetha Balakrishna, [†] Priyam Mukherjee, [††] Hyun Young Jung, [¥] Ketaki Samanta[⁋] and Debasis Ghosh[†, ¥ *]

[†]*Centre for Nano and Material Sciences, Jain (Deemed-to-be University), Jain Global Campus, Kanakapura, Bangalore, Karnataka, India – 562112*

[††]*Department of Physics, Indian Institute of Technology Guwahati, Guwahati, Assam, 781039 India*

[¥]*Department of Energy Engineering, Gyeongsang National University, Jinju-si, Gyeongnam 52725, South Korea*

[⁋]*Department of Materials Engineering, Indian Institute of Science, Bangalore, Karnataka 560012, India.*

***Corresponding authors:**

DG: g.debasis@jainuniversity.ac.in; debasisghosh88@gmail.com

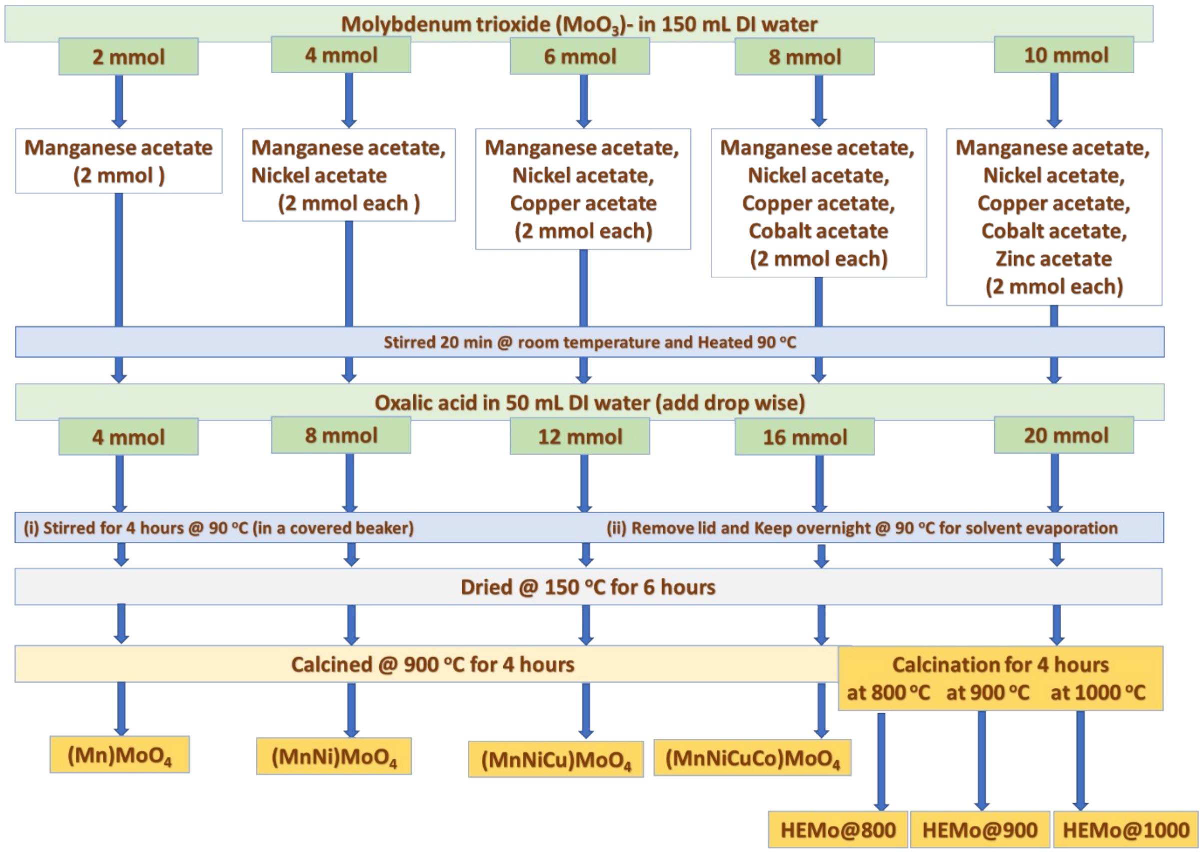

Figure S1. Schematic illustration of the synthesis process of metal molybdates.

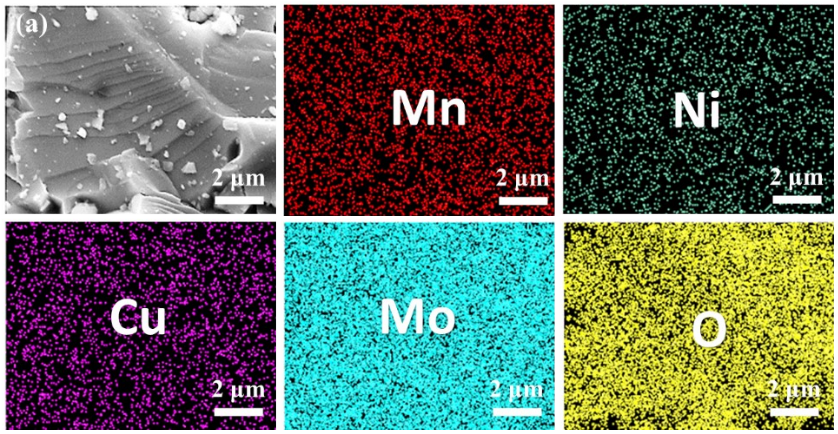

Figure S2. EDX elemental mapping of $(MnNiCu)MoO_4$: mapping was carried out on the whole area of Figure (a), and the surface mapping of Mn, Ni, Cu, Mo, and O elements with corresponding % are shown.

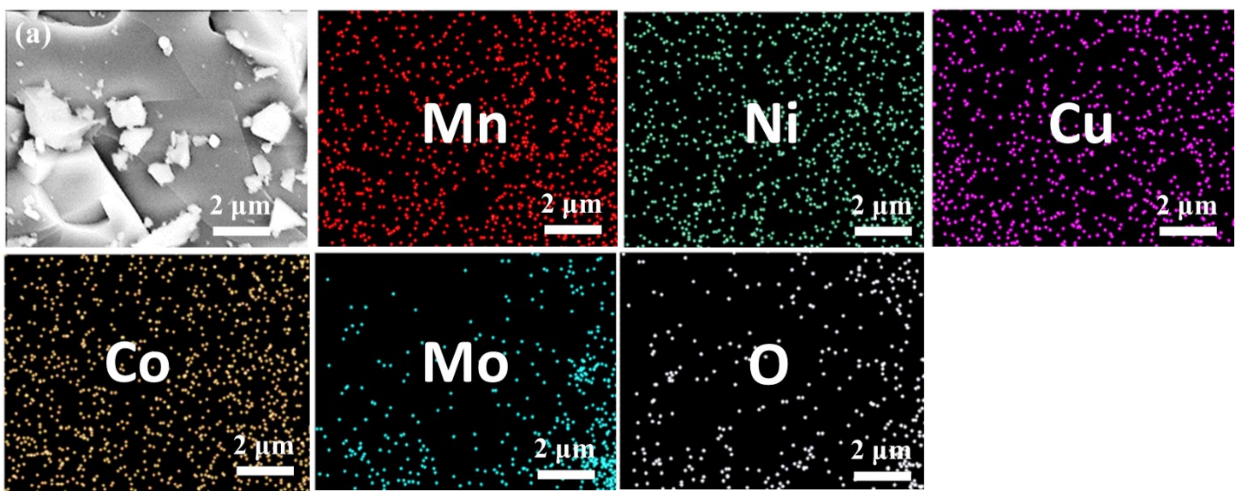

Figure S3. EDX elemental mapping of $(MnNiCuCo)MoO_4$: mapping was carried out on the whole area of Figure (a), and the surface mapping of Mn, Ni, Cu, Co, Mo, and O elements with corresponding % are shown.

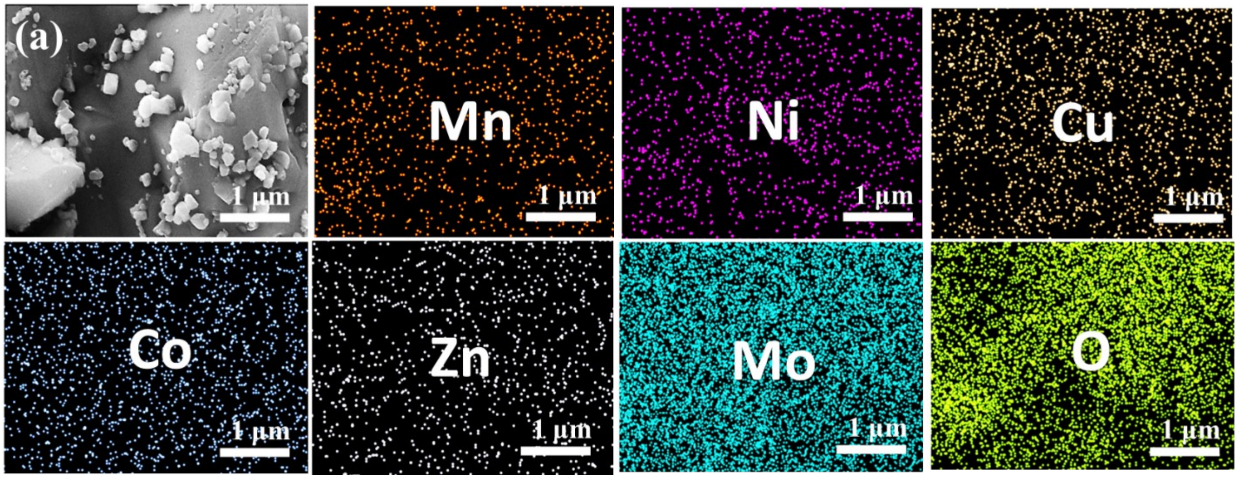

Figure S4. EDX elemental mapping of HEMo@800: mapping was carried out on the whole area of Figure (a), and the surface mapping of Mn, Ni, Cu, Co, Zn, Mo, and O elements with corresponding % are shown.

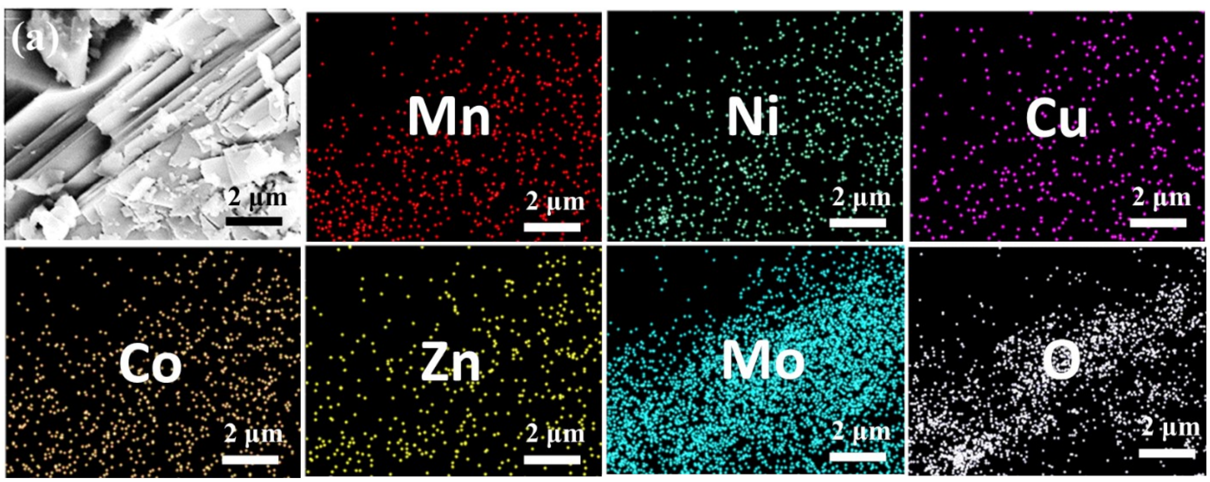

Figure S5. EDX elemental mapping of HEMo@1000: mapping was carried out on the whole area of Figure (a), and the surface mapping of Mn, Ni, Cu, Co, Zn, Mo, and O elements with corresponding % are shown.

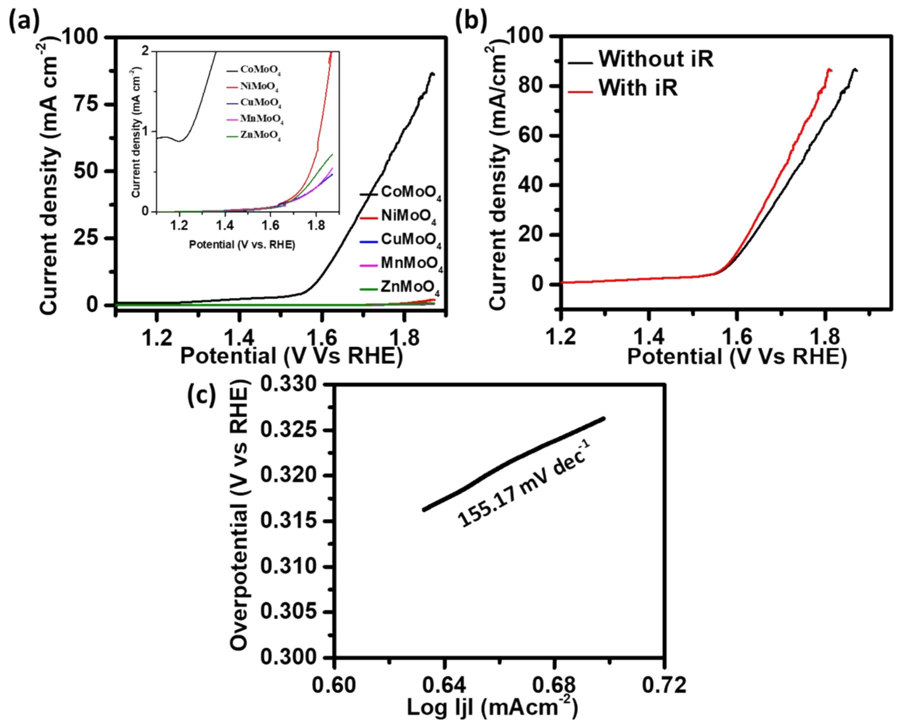

Figure S6. (a) Comparison of LSV curves for different mono metal molybdates; (b) With and without *iR* corrected OER polarization curves of $CoMoO_4$ and (c) Tafel plot of $CoMoO_4$ obtained from *iR* corrected LSV plot.

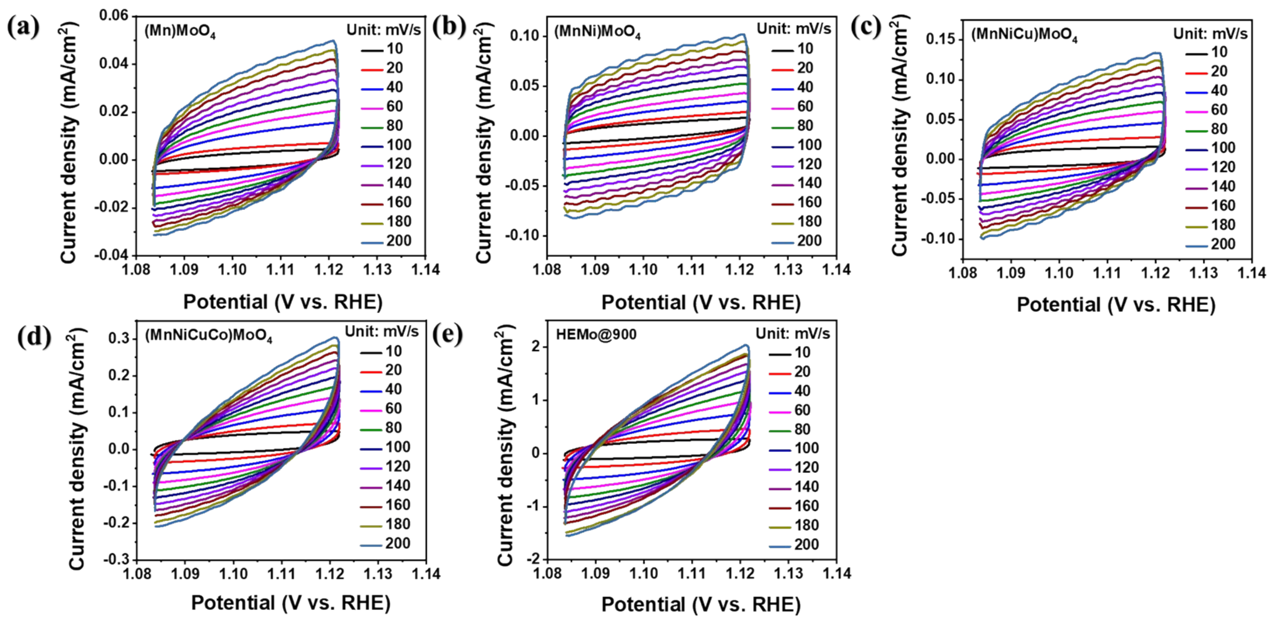

Figure S7. Non-faradaic CV curves of (Mn)Mo$_4$ (a), (MnNi)MoO$_4$ (b), (MnNiCu)Mo$_4$ (c), (MnNiCuCo)MoO$_4$ (d), and HEMo@900 (e) at different scan rates.

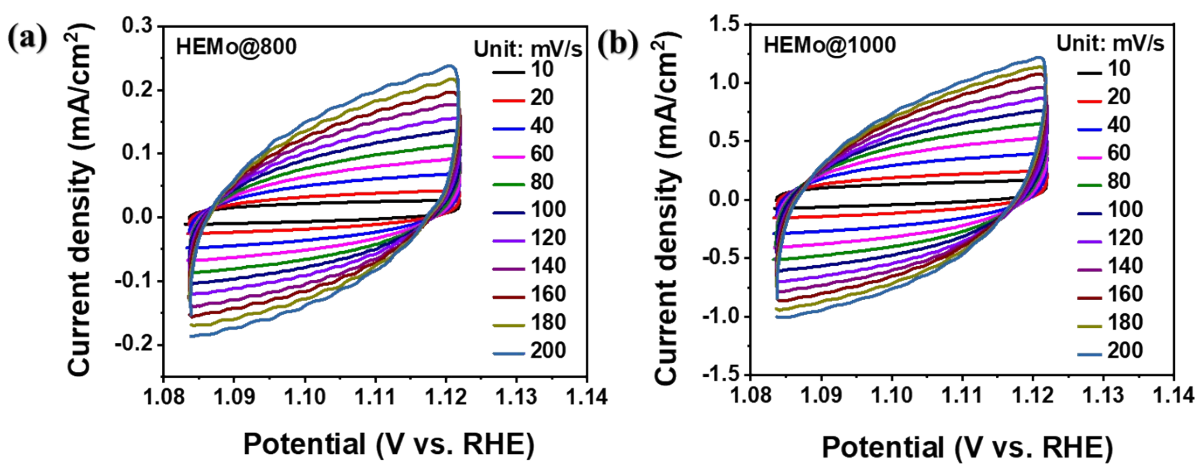

Figure S8. Non-faradaic CV curves of HEMo@800 (a) and HEMo@1000 (b) at different scan rates.

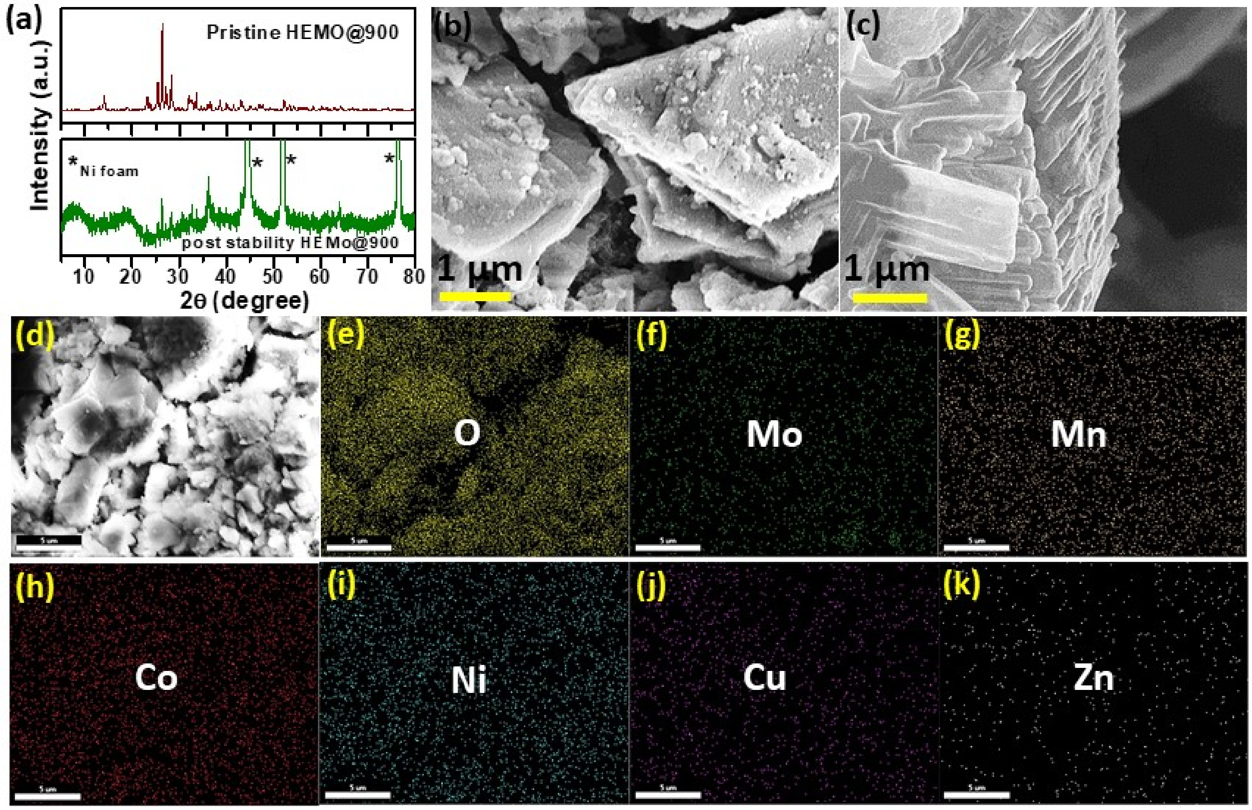

Figure S9 Post stability study of HEMo@900 electrocatalyst: (a) XRD pattern; FESEM images of the HEMo@900 at different magnifications (b-c) and EDX elemental mapping of image (d) showing the uniform distribution of the elements (e) O, (f) Mo, (g) Mn, (h) Co, (i) Ni, (j) Cu and (k) Zn.

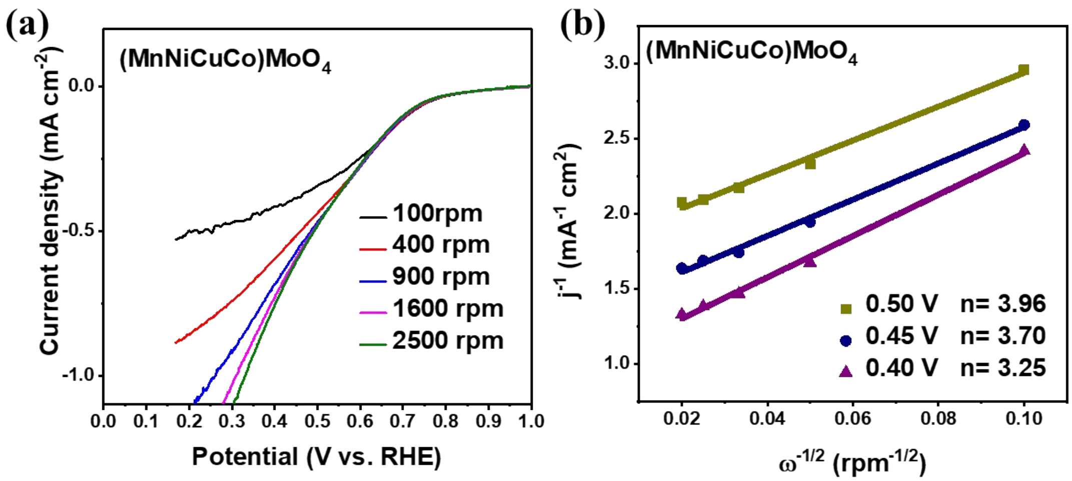

Figure S10: ORR polarization plots of the (MnNiCuCo)MoO_4 in O_2 saturated 1 M KOH at different RPM values, and (b) K-L plot as obtained from the ORR polarization curves.

Table S1: Reflections (hkl) and corresponding 2Θ diffraction angles.

	JCPDS 01-072-0285 - $MnMoO_4$	MnMoO4	(MnNi) MoO_4		JCPDS 00-021-0868- $CoMoO_4$	(MnNiCu) MoO_4	(CoMnNiCu) MoO_4	HEMo @ 900	HEMo @ 1000	HEMo @ 800
Reflection (hkl)	2Θ (degree)	2Θ (degree)	2Θ (degree)	Reflection (hkl)	2Θ (degree)	2Θ (degree)	2Θ (degree)	2Θ (degree)	2Θ (degree)	2Θ (degree)
(110)	12.801	12.7868	13.074	(001)	13.204	13.1466	13.1849	13.1871	13.139	13.1241
(-201)	18.726	18.721	18.9599	(-201)	19.071	18.9318	18.9597	18.8974	18.8027	18.7981
(021)	22.73	22.7407	23.1188	(021)	23.329	23.1854	23.2932	23.2781	23.2426	23.2279
(201)	24.709	24.6659	25.1831	(201)	25.502	25.358	25.4632	25.397	25.3505	25.385
(220)	25.766	25.7602	26.2602	(002)	26.507	26.3487	26.4703	26.3876	26.3448	26.3628
(002)	25.969	25.9599	27.0101	(-112)	27.25	27.1444	27.2242	27.1873	27.1167	27.168

(-112)	26.685	26.7079	27.3322	(-311)	28.401	28.3439	28.4231	28.3455	28.3784	28.3194
(-311)	27.766	27.7665	28.1796	(-131)	32.09	31.9578	32.07	32.0441	32.6248	32.0089
(112)	31.256	31.2264	31.7698	(-222)	33.706	33.5274	33.6543	33.6026	33.5761	33.5916
(-222)	33.046	33.0354	33.4526	(040)	38.871	38.4655	38.6447	38.6536	38.6138	38.6078
(400)	35.71	35.6457	36.3044	(222)	41.624	41.379	41.5444	41.5179	41.3892	41.4462
(040)	37.785	37.7259	38.4695	(241)	47.02	47.0022	47.0366	47.5759	47.5036	47.1037
(-113)	39.078	39.0147	39.8084	(-204)	52.07	52.1428	52.1889	52.1602	52.1126	52.1066
(222)	40.449	40.3448	41.1448	(-440)	54.547	53.4041	53.3543	53.2541	53.2895	53.1235
(241)	45.673	45.79	46.5994	(024)	58.438	57.9528	58.3505	58.348	58.2677	58.3098
(-204)	51.218	51.1844	51.793	(-424)	60.415	60.2242	59.6117	61.2177	61.0493	61.1299
(440)	52.965	52.8436	53.9643							
(024)	57.064	56.9706	57.8946							
(-424)	59.324	59.2956	59.9932							

Table S2: Comparison of different bifunctional (ORR/OER) electrocatalytic performances with HEMo@900 material.

Materials	**Electrolyte**	**Catalyst loading (mg cm^{-2})**	**OER**		**Electrolyte**	**Catalyst loading (mg cm^{-2})**	**ORR**	
Material [Ref]			**Overpotential (mV) @10 mA cm^{-2}**	**Tafel slope (mV dec^{-1})**			**Half-wave potential (V *vs.* RHE)**	**Tafel slope (mV dec^{-1})**
This work (HEMo@900)	**1 M KOH**	**0.35**	**318**	**49.45**	**1 M KOH**	**0.38**	**0.74**	**93.09**
FeNC [1]	0.1 M KOH	0.8	320	305	0.5 M H_2SO_4	0.8	0.72	--
$MnFe_2O_4$ [2]	0.1 M	0.15	590	--	0.1 M	0.15	0.71	71

	KOH				KOH			
$NiFe_2O_4$ [2]	1 M KOH	0.15	410	--	0.1 M KOH	0.15	0.68	57
$CoFe_2O_4$ [2]	0.1 M KOH	0.15	410	--	0.1 M KOH	0.15	0.73	53
$CuCo_2S_4$ NSs [3]	0.1 M KOH	0.2	287	46	0.1 M KOH	0.2	0.70	73
Nickel Cobaltite [4]	0.1 M KOH	0.20	400	70	0.1 M KOH	0.20	0.73	90
$MnFe_2O_4$ [5]	0.1 M KOH	0.0306	540	--	0.1 M KOH	0.0306	0.72	--
MnO_2 [6]	0.1 M KOH	0.204	610	60	0.1 M KOH	0.204 mg cm−2	0.56	256
ns$LaNiO_3$/NC [7]	0.1 M KOH	0.051	430	42	0.1 M KOH	0.051	0.64	--
De-$Li(Ni_{0.2}Co_{0.6}Mn_{0.2})O_2$ [8]	0.1 M KOH	0.118	310	36	0.1 M KOH	0.118	0.71	--
$MnCo_2O_{4.5}$ [9]	0.1 M KOH	0.2756	410	144	0.1 M KOH	0.2756	0.72	--
LSMI [10]	0.1 M KOH	0.2	440	103	0.1 M KOH	0.2	0.73	--
$BaFe_{0.8}Co_{0.2}O_{2.09}(OH)_{0.78}$ [11]	0.1 M KOH	0.3	450	190	0.1 M KOH	0.3	0.675	84
LT-$Li_{0.5}CoO_2$ [12]	1 M KOH	0.25	320	60	0.1 M KOH	0.25	0.64	--
H_2-CMNO [13]	0.1 M KOH	0.4	550	98	0.1 M KOH	0.4	0.68	80
LSMF [14]	1 M KOH	0.305	610	230	0.1 M KOH	0.305	0.73	137
LC5N5 [15]	1 M KOH	--	400	73.9	0.1 M KOH	--	0.67	112
PBSCF-NF [16]	0.1 M KOH	--	300	81	0.1 M KOH	0.796	0.69	98
$Co_3FeS_{1.5}(OH)_6$ [17]	1 M KOH	--	358	79	0.1 M KOH	--	0.721	96
LFP [18]	1 M KOH	0.255	460	50	0.1 M KOH	0.255	0.66	64
DCN-M [19]	1 M KOH	0.2	350	68.83	0.1 M KOH	0.2	0.864	105.68
Co/N-Pg [20]	0.1 M KOH	0.35	--	70	0.1 M KOH	0.35	0.82	61

Co NP/NC [21]	0.1 M KOH	0.5	430	--	0.1 M KOH	0.5	0.8	--
Co@CNTs [22]	0.1 M NaOH	0.450	340	72	0.1 M KOH	0.450	0.9	78
Co@NSCNT [23]	0.1 M KOH	--	520	154	0.1 M KOH	--	0.906	--
FeCo/NSC [24]	0.1 M KOH	0.42	325	99.15	0.1 M KOH	0.42	0.82	69.75
Co/MoC@N-C [25]	1 M KOH	0.850	290	90	1 M KOH	0.850	0.824	93.26
CoO_x/CeO_2/RGO [26]	0.1 M KOH	0.35	360	86	0.1 M KOH	0.35	0.83	54
$ZnCoMnO_4$/N-rGO [27]	0.1 M KOH	--	450	158	0.1 M KOH	--	0.83	75
G@N–MoS_2 [28]	0.1 M KOH	0.25	390	--	0.1 M KOH	0.25	0.716	--
AuIr/C [29]	1 M KOH	--	394	--	0.1 M NaOH	--	0.774	--
$NiCoO_2$/CNTs [30]	0.1 M KOH	0.3	430	156	0.1 M KOH	0.3	0.67	--
Ni_3FeN/NRGO [31]	0.1 M KOH	0.1	400	--	0.1 M KOH	0.1	0.70	--
Ni/NiO/$NiCo_2O_4$/N–CNT–As [32]	0.1 M KOH	0.240	280	45	0.1 M KOH	0.240	0.74	--
FeO_x@N-PHCS [33]	0.1 M KOH	0.25	340	162	0.1 M KOH	0.25	0.86	--

References:

1. K. Mamtani, D. Jain, A. C. Co and U. S. Ozkan, *Energy & Fuels*, 2017, **31**, 6541-6547.
2. C. Si, Y. Zhang, C. Zhang, H. Gao, W. Ma, L. Lv and Z. Zhang, *Electrochimica Acta*, 2017, **245**, 829-838.
3. Y. Li, J. Yin, L. An, M. Lu, K. Sun, Y.-Q. Zhao, F. Cheng and P. Xi, *Nanoscale*, 2018, **10**, 6581-6588.
4. D. U. Lee, M. G. Park, Z. P. Cano, W. Ahn and Z. Chen, *ChemSusChem*, 2018, **11**, 406-414.
5. Y. Zhou, Y. Du, S. Xi and Z. J. Xu, *Electrocatalysis*, 2017, **9**, 287-292.
6. K. Selvakumar, S. M. S. Kumar, R. Thangamuthu, P. Rajput, D. Bhattacharyya and S. N. Jha, *ChemElectroChem*, 2018, **5**, 3980-3990.
7. W. G. Hardin, D. A. Slanac, X. Wang, S. Dai, K. P. Johnston and K. J. Stevenson, *The Journal of Physical Chemistry Letters*, 2013, **4**, 1254-1259.
8. Y. Zou, G. Chang, Y. Jia, R. Cai, S. Chen, Y. Xia, W. Theis, D. Yang and X. Yao, *Energy Storage Materials*, 2018, **15**, 202-208.

9. Z. Bai, J. Heng, Q. Zhang, L. Yang and F. Chang, *Advanced Energy Materials*, 2018, **8**.
10. L. Yan, Y. Lin, X. Yu, W. Xu, T. Salas, H. Smallidge, M. Zhou and H. Luo, *ACS Applied Materials & Interfaces*, 2017, **9**, 23820-23827.
11. A. I. Waidha, L. Ni, J. Ali, M. Lepple, M. Donzelli, S. Dasgupta, S. Wollstadt, L. Alff, U. I. Kramm and O. Clemens, *Journal of Materials Chemistry A*, 2020, **8**, 616-625.
12. T. Maiyalagan, K. A. Jarvis, S. Therese, P. J. Ferreira and A. Manthiram, *Nature Communications*, 2014, **5**.
13. Y.-Q. Lyu and F. Ciucci, *ACS Applied Materials & Interfaces*, 2017, **9**, 35829-35836.
14. R.-h. Yuan, Y. He, W. He, M. Ni and M. K. H. Leung, *Applied Energy*, 2019, **251**.
15. H. Wang, W. Xu, S. Richins, K. Liaw, L. Yan, M. Zhou and H. Luo, *Electrochimica Acta*, 2019, **296**, 945-953.
16. Y. Bu, O. Gwon, G. Nam, H. Jang, S. Kim, Q. Zhong, J. Cho and G. Kim, *ACS Nano*, 2017, **11**, 11594-11601.
17. H. F. Wang, C. Tang, B. Wang, B. Q. Li and Q. Zhang, *Advanced Materials*, 2017, **29**.
18. Z. Li, L. Lv, J. Wang, X. Ao, Y. Ruan, D. Zha, G. Hong, Q. Wu, Y. Lan, C. Wang, J. Jiang and M. Liu, *Nano Energy*, 2018, **47**, 199-209.
19. D. Chen, W. Cao, J. Liu, J. Wang, X. Li and L. Jiang, *Journal of Energy Chemistry*, 2021, **59**, 47-54.
20. Y. Tian, L. Xu, J. Bao, J. Qian, H. Su, H. Li, H. Gu, C. Yan and H. Li, *Journal of Energy Chemistry*, 2019, **33**, 59-66.
21. J. Zhao, F. Rong, Y. Yao, W. Fan, M. Li and Q. Yang, *Journal of Energy Chemistry*, 2018, **27**, 1261-1267.
22. J. Jiao, Y. Pan, B. Wang, W. Yang, S. Liu and C. Zhang, *Journal of Energy Chemistry*, 2021, **53**, 364-371.
23. T. Oh, K. Kim and J. Kim, *Journal of Energy Chemistry*, 2019, **38**, 60-67.
24. S. Chang, H. Zhang and Z. Zhang, *Journal of Energy Chemistry*, 2021, **56**, 64-71.
25. H. Huang, L. Kong, M. Liu, J. He, W. Shuang, Y. Xu and X.-H. Bu, *Journal of Energy Chemistry*, 2021, **59**, 538-546.
26. H. Zhong, L. Alberto Estudillo-Wong, Y. Gao, Y. Feng and N. Alonso-Vante, *Journal of Energy Chemistry*, 2021, **59**, 615-625.
27. W. Liu, D. Rao, J. Bao, L. Xu, Y. Lei and H. Li, *Journal of Energy Chemistry*, 2021, **57**, 428-435.
28. C. Tang, L. Zhong, B. Zhang, H.-F. Wang and Q. Zhang, *Advanced Materials*, 2018, **30**.
29. L. Yuan, Z. Yan, L. Jiang, E. Wang, S. Wang and G. Sun, *Journal of Energy Chemistry*, 2016, **25**, 805-810.
30. L. Ma, H. Zhou, Y. Sun, S. Xin, C. Xiao, A. Kumatani, T. Matsue, P. Zhang, S. Ding and F. Li, *Electrochimica Acta*, 2017, **252**, 338-349.
31. Y. Fan, S. Ida, A. Staykov, T. Akbay, H. Hagiwara, J. Matsuda, K. Kaneko and T. Ishihara, *Small*, 2017, **13**.
32. N. Ma, Y. Jia, X. Yang, X. She, L. Zhang, Z. Peng, X. Yao and D. Yang, *Journal of Materials Chemistry A*, 2016, **4**, 6376-6384.
33. R. Hao, J.-T. Ren, X.-W. Lv, W. Li, Y.-P. Liu and Z.-Y. Yuan, *Journal of Energy Chemistry*, 2020, **49**, 14-21.